

Molecular electronics exploiting sharp structure in the electrode density-of-states. Negative differential resistance and Resonant Tunneling in a poled molecular layer on Al/LiF electrodes.

Z.H. Lu,¹ M.W.C. Dharma-wardana*,² R.S. Khangura,¹ Marek Z. Zgierski,² and Douglas Ritchie²

¹*Department of Materials Science and Engineering, University of Toronto
184 College Street, Toronto, Ontario M5S 3E4*

²*National Research Council of Canada, Ottawa, Canada. K1A 0R6*

(Dated: February 2, 2008)

Density-functional calculations are used to clarify the role of an ultrathin *LiF* layer on *Al* electrodes used in molecular electronics. The *LiF* layer creates a sharp density of states (DOS), as in a scanning-tunneling microscope (STM) tip. The sharp DOS, coupled with the DOS of the molecule leads to negative differential resistance (NDR). Electron transfer between oriented molecules occurs *via* resonant tunneling. The $I - V$ characteristic for a thin-film of tris (8-hydroxyquinoline)-aluminum (*AlQ*) molecules, oriented using electric-field poling, and sandwiched between two *Al/LiF* electrodes is in excellent agreement with theory. This molecular device presents a new paradigm for a convenient, robust, inexpensive alternative to STM or mechanical break-junction structures.

PACS numbers: PACS Numbers: 05.30.Fk, 71.10.+x, 71.45.Gm

Introduction. An intense effort has been directed to the practical realization of molecular electronics (ME) [2, 3, 4], since conventional silicon technology is approaching the limit of “Moore’s law” [5]. The advantages of ME are related to properties unique to molecules. Molecules are nanostructures with near-perfect topological linkages. The disruption in surface topology involved in microfabrication is a limiting factor in using inorganic materials such as GaAs[6]. The energy scales associated with molecules (unlike, say, quantum dots) make them capable of operating at room temperature. Mechanically controllable break junctions[7] and molecular contacts using scanning-tunneling microscope (STM) tips have been considered[2]. However, molecule-atom contacts may sometimes take disruptive pathways that lead to fragmentation of the metal contacts or the molecule itself[8, 9]. Assuming non-disruptive contacts could be made, an additional step of coherently connecting many molecules together requires exotic tools. Hence the future of ME depends on surmounting the theoretical and practical challenge of realizing robust, reproducible, inexpensive devices.

In this study we show both theoretically and experimentally that a practical, robust realization of molecular-NDR characteristics is possible by exploiting two important features, *viz.*, (i) the special characteristics of the density of states (DOS) of *LiF* thin films deposited on *Al*, and (ii) The possibility of aligning molecules by electric poling, i.e, cooperatively aligning the molecules along the field direction when an external electric field is applied. Examples of electric poling are common in the field of liquid crystals and non-linear optical polymers[10]. The experimental $I - V$ characteristic inclusive of NDR effects is found to be in agreement with our calculations.

The device structure.—The experimental structure was fabricated in a cluster tool having a central distribution chamber, a load-lock chamber, a plasma cleaning cham-

ber, a sputtering chamber, an organic molecular-growth chamber, and a metallization chamber. Figure 1 shows the layer sequence used. A 2”x2” *Si* substrate with ~ 70 nm of oxide was cleaned by oxygen plasma and then transferred to the metallization chamber for electrode deposition. The bottom *Al* electrode (1 mm wide and 2 mm spacing between adjacent electrodes) was fabricated by thermal evaporation through a shadow mask in the metallization chamber. The top electrode was similarly deposited but the electrode lines run orthogonal to the bottom ones. The interception area (1mm x1mm) forms one individual device. One hundred such testing devices were fabricated on a 2”x2” silicon substrate. After the deposition of the bottom electrode, the wafer was transferred to the organic molecular-growth chamber for *AlQ* deposition. Electronic grade *AlQ* was purchased from Kodak. *AlQ* films were fabricated using a low-temperature K-cell with an alumina crucible. Thicknesses of 50-200 nm have been tried and 100 nm *AlQ* was optimal with good electrical properties and high yield (>90%). The 100 nm *AlQ* thin-film devices used *Al* electrodes having an ultrathin layer of (~ 0.2 - 0.3 nm) *LiF* between *Al* and *AlQ* [11]. The crucial role of the *LiF* will be discussed below. After the deposition of the top electrode, the device was sealed off from the ambient using a 120 nm silicon oxide passivation layer. This passivation layer is very critical to obtaining reproducible results.

Measurements and results.—The current-voltage ($I - V$) measurements were conducted using a HP4140B meter with a Materials Development probe station. Figure 1 (lower panel) shows $I - V$ characteristics of one typical device before poling (dashed line) at 298 K and after poling (solid line) at 255 K. The electric poling was made by sweeping the applied voltage from the starting poling voltage V_p onwards with a dwell time of 1 second per voltage point, in the same mode of $I - V$ measurement. The starting V_p is ~ 13 V at 298K and ~ 10 V at

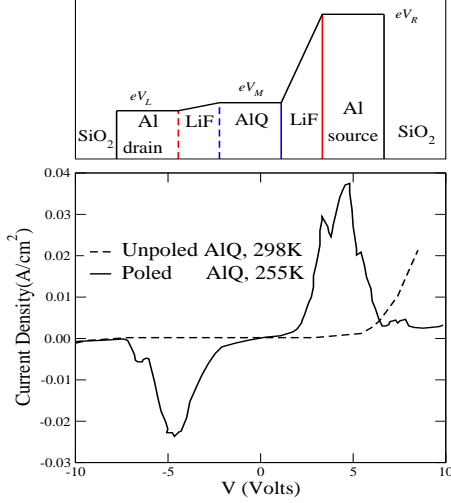


FIG. 1: Top: Schematic of the molecular device, and voltage profile in the device for poled AlQ. The "bottom" Al-electrode is at the right end. Lower panel: $I - V$ characteristics of the device without electric poling and with poling where NDR structures arise.

255K. The maximum poling voltage is ~ 18 V. It is quite clear that after electric poling, sharp NDR peaks near -3 V and +3V were developed. The peak structures are very similar to those observed on a single molecule or self-assembled molecular monolayer[3, 7]. We also found that the NDR peak can be erased by passing a high current at a higher positive bias-voltage, and the erased peak can be re-generated by poling. It can be repeated many times on some devices. Because there are no strong primary bonds between molecules, the molecular alignment may be readily destroyed by thermal effects. Nevertheless we found that over 90% of the device showed similar characteristics. Similar, sporadic and unexplained observations of NDR from AlQ has been reported in the literature[12]. Here we present controlled observations whose origin is quantitatively explained.

Theoretical considerations.— The electrode (see Fig. 1) chemical potentials are μ_L , and μ_R , with $-|e|V = \mu_L - \mu_R$, where $V = V_R - V_L$ is the applied potential. The electron flow involves (i) electron injection into the molecular layer at the right, denoted by $R \rightarrow M$, and described by a transmission function T_{RM} which is essentially the joint density of states of the electrode surface and the molecular layer, weighted by a matrix element. (ii) Transfer of carriers from molecule to molecule, $M \rightarrow M$, described by T_{MM} and finally, (iii) transfer from the molecular layer to the left electrode, $M \rightarrow L$, described by T_{ML} .

We begin by a qualitative discussion.

The interaction between Al surfaces and organic molecules like AlQ has been studied extensively[13, 14].

The AlQ molecules placed directly in contact with the Al surface is known to undergo reactions (e.g., between Al and the quinolate-O). Clearly, an important role of the LiF is in shielding the molecules against such reactions. Various indirect interfaces, e.g. Al/X/AlQ, where X may be, say, LiF, CaF_2 , SiO_2 etc., have been examined. It has been found that a few atomic layers of LiF separating the AlQ from the Al electrode produces a striking improvement in the $I - V$ characteristics and lowers the threshold for electron injection. Although this system has been extensively investigated, a clear explanation of how LiF helps has not been forthcoming.

We show that the Al/LiF-electrode DOS is like a δ -function sitting on the slowly varying DOS of the Al substrate. The DOS of the AlQ molecule is also found to have a strong sharp feature (SF) in the unoccupied manifold of states (UMS). At the appropriate bias, electrons are injected into the SF of the UMS. Unlike injection into the lowest unoccupied state ("LUMO") which is affected by the Coulomb blockade and the need for molecular rearrangement, injection to a higher energy UMS couples only weakly to the ground-state electron distribution. The injected electrons rapidly migrate in the poled molecular film by resonant tunneling. Hence the inter-molecular transmission function T_{MM} is essentially unity. Finally, electrons arriving at the drain electrode are in an excited state above the Fermi energy of the Al electrode, and can resonantly tunnel into the slowly varying unoccupied DOS of the Al substrate. This resonant process also involves a negligible potential drop if the intervening LiF layer is atomically thin. Thus essentially all the potential drop occurs at the injection electrode (see Fig.1, top panel) where there is also an "empty" region (not shown in the figure) between the LiF surface and the first AlQ layer. All these lead to an effective tunneling length s which will appear in the matrix element connecting the electrode states and the AlQ states. Thus the potential profile in Fig. 1 is rather schematic and does not show the LiF - AlQ tunneling gap which is found from our calculations (see below) to be about ~ 0.1 nm, while the LiF layer is about 0.2-0.3 nm. We have, to leading order,

$$T_{RM}(E, V) = (2\pi)^2 |A_{RM}(V)|^2 \rho_R(E - eV) \rho_M(E) \quad (1)$$

Here A_{RM} is the matrix element connecting the molecule and the electrode, and ρ_R , ρ_M are the DOS of the right electrode (R) and the molecule (M) respectively. Given our previous conclusion that T_{MM} , and T_{ML} are resonant processes of the order of unity, the current is effectively determined by T_{RM} . The bias dependence of $A_{RM}(V)$ can be neglected only if two sharp features in the two DOS functions are involved. However, the bias dependence of $A_{RM}(V)$ is important, and this can be included by evaluating the matrix element as in Lang[15].

A standard Fermi Golden-rule analysis, or a Landauer-Büttiker approach may be used to write an expression for the current I in terms of the transmission function

$T(E, V)$.

$$I = 2\sigma_0 \int_{-\infty}^{\infty} dE T(E, V) [f(E - \mu_R) - f(E - \mu_L)] \quad (2)$$

Here σ_0 is the quantum of conductance $e^2/h = 1$ in atomic units, which corresponds to a resistance of $12.9 K\Omega$ in conventional units. The Fermi factors are effectively step functions even at room temperature. Thus the dominant contribution to the current is given by:

$$I(V) = A \int_{\mu_L}^{\mu_R} dE \rho_R(E - eV) \rho_M(E) e^{-2s\{2(E - W) + eV\}^{1/2}} \quad (3)$$

where A is a numerical factor and $\mu_L = E_F$ is the Fermi energy, while $\mu_R = E_F + eV$. Here s is an effective tunneling length linking the molecule and the Al/LiF electrode, and W is the workfunction[15]. These are treated as parameters of the problem. The main effect of higher temperatures comes in via a convolution of the T_{MM} which involves molecular Debye-Waller effects. We have neglected such effects.

The left electrode was made by depositing LiF and then Al on AlQ , and hence follows the reverse of the fabrication sequence used for the right electrode. However, the electronic processes in the device are essentially symmetric, with slightly different values for s , W etc. When the bias is reversed, the carrier processes reverse direction. This is different to the situation in Au -thiol-STM devices where the thiol is chemically attached to the Au electrode. Then NDR is obtained by having two potential drops at the two electrodes[3]. Also, unlike in the Au -thiol-STM system, the AlQ molecules are shielded from the Al electrode by the LiF overlayers, and the main potential drop occurs at the injector LiF dielectric layer, at the empty region between the LiF surface and the first AlQ molecular layer. This is estimated to be about ~ 1.2 Angstroms and plays the role of a tunneling length.

Density of states of the Al/LiF electrode.— Bulk LiF and bulk Al both have FCC structures and are very nearly lattice matched. While Al is a very good metal, LiF is a large-bandgap insulating ionic crystal. We have carried out first-principles density functional calculations to simulate $Al/(LiF)_n$ where the number of atomic planes n was varied from 1 to 4 to give LiF -overlayers. The crystallographic details of the experimental Al surface is unknown. We have carried out calculations with the LiF layers arranged along $[001]$ as well as along $[111]$ directions with very similar results. The Al substrate was modeled with 6 planar layers of Al in the growth direction, and periodically continued in the $x - y$ directions. The last layer of Al and the LiF layer were geometry optimized using standard energy minimization methods available with the VASP plane-wave code[16]. The simulation cell (SC) included five vacuum layers to separate the Al substrate from the LiF . DOS calculations were done using an $11 \times 11 \times 11$ Monkhorst-Pack k -sampling scheme. The Al atomic layer adjacent to the

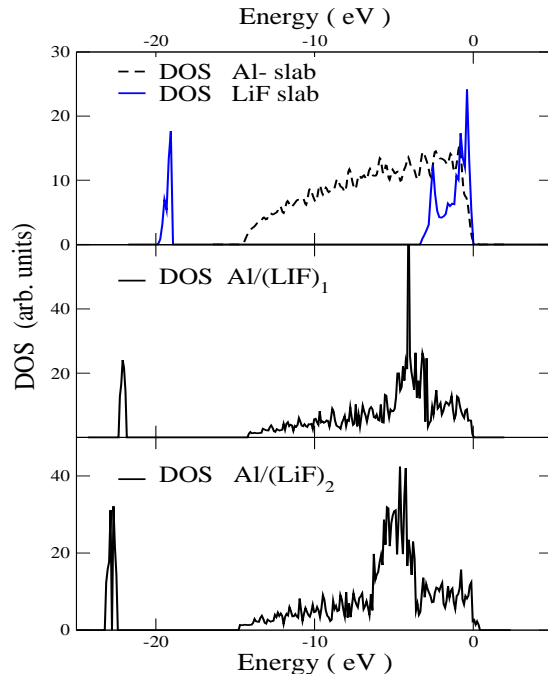


FIG. 2: The top panel contains the occupied-state DOS of bulk- Al and bulk- LiF , with both Fermi levels set to zero. The lower two panels show the DOS with a single monoatomic layer of LiF , and 2 atomic layers of LiF , deposited on Al and structure optimized by total-energy minimization.

LiF suffers virtually no reconstruction, while the F and Li atoms which were initially coplanar in the (001) layers, reconstruct in opposite directions, with the F^- moving inwards, towards the Al layer, while the Li^+ ions move outwards, along the growth axis. This reconstruction is very small ($\sim 0.1A$). Similar effects, as well as metal-induced surface states, have been reported in $Cu/LiCl$ and related systems recently[17]. A crucial effect of the LiF layer on Al is seen in Fig.2. The DOS of Al by itself, LiF by itself, and in the combined structure $Al/(LiF)_n$ are shown in Fig. 2, all referred to the same Fermi level set to zero for clarity. It is clear that a sharp structure (similar to that in the DOS of an STM tip) is produced in the $Al/(LiF)_n$ system if n is small. Thus, if an Al electrode has an *atomically thin* overlayer of LiF , we have an injection DOS similar to those created using mechanical break junctions or STM-tip molecular contacts.

The calculation of the transmission function $T(E, V)$ requires the DOS of the AlQ molecule as well. Here a cluster-type calculation is appropriate, while it would *not* be appropriate for the Al metallic layers. The electronic structure of the AlQ molecule and the AlQ^- negative ion were calculated using the Gauss98 code at the B3LYP/3-21G* level[18, 19]. These calculations included geometry optimization together with total energy minimization and state of the art gradient cor-

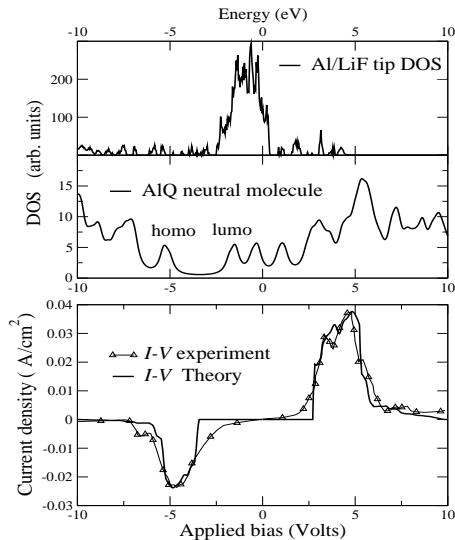


FIG. 3: Top: the *Al/LiF* “tip” like DOS with the *Al* DOS subtracted out. Middle panel shows the DOS of the neutral *AlQ* molecule. Lower panel: *I* – *V* characteristics of the device compared with theory.

rected exchange-correlation functionals. Density of states (DOS) curves were constructed using a 0.25 eV Lorentz broadening of the one-particle eigenenergies. These calculations reveal a highest occupied molecular orbital (HOMO) at -5.02 eV and a lowest unoccupied molecular orbital (LUMO) at -1.79 eV, while the optical gap was previously calculated by us [20] to be 2.7 eV.

*Comparison of calculated and observed *I* – *V* characteristics.*– The analysis leading to Eq. 3 showed that the *I* – *V* characteristic would depend on the main features of the DOS of the molecular film, i.e., the molecule itself as we have a simple chemically uncoupled array of molecules. In fig. 3, top panel, we present the “tip-like” DOS of the *Al/LiF* layer, with the back-

ground *Al* density of states subtracted off (e.g, bottom panel of Fig.2 minus the *Al*-slab DOS from the top panel of Fig.2). The DOS of the *AlQ* molecule is shown in the middle panel. The bottom panel shows the experimental *I* – *V* data at 255 K compared with the theoretical result obtained from Eq. 3. The experimental *I* – *V* agreed with the theory for a workfunction $W \sim 4.6 - 4.9\text{eV}$, and with the effective tunneling length $s \sim 0.8 - 1.3$ Angstroms. The numerical factor A was ~ 0.001 .

Discussion.– In the usual picture (*not used by us*) of electron transport across the A/*AlQ*/B structures under bias, it is assumed that an electron is injected from the source into the LUMO of the *AlQ* molecule, converting it to a transient *AlQ*^{−*} anion. This involves Coulomb blockade, rearrangement of bond lengths, bond angles etc., to give the actual *AlQ*[−] anion. The carrier then hops to a neighboring *AlQ* molecule and moves towards the drain electrode. There is no resonant transfer possible not only because the *AlQ* molecules are not properly oriented, but also because the available LUMO states are not in resonance with the *AlQ*[−] eigenstate containing the carrier electron. The *I* – *V* characteristics show no NDR effects.

In contrast, in the structure discussed here, the molecules in the electric-field poled *AlQ* layer form an oriented array. The electron is injected to an unoccupied high-energy state by the sharp DOS structure of the *Al/LiF* electrode. The electron reaches the drain electrode by inter-molecular resonant transfer. Since only high-energy unoccupied states are invoked, this process does not involve significant Coulomb blockade or bond-rearrangement bottlenecks. The device is robust, easy to make and works at ambient temperatures.

Conclusion– We have shown, experimentally and theoretically, that a robust room-temperature molecular device, showing *I* – *V* characteristics similar to those obtained in STM-based molecular devices, can be fabricated using *Al/LiF* electrodes and a poled molecular film. New insight into the role of *LiF* overlayers in electrode processes is also presented.

-
- [1] * electronic address: chandre.dharma-wardana@nrc.ca
 - [2] For references to early work, see N. D. Lang, Phys. Rev. B, **52**, 5335 (1995)
 - [3] S. Datta et al., Phys. Rev. Lett. **79**, 2530 (1997); M. Di Ventra et al., *Ibid* **84**, 979 (2000); E. G. Emberley et al., Phys. Rev. B **58**, 10911 (1998); H. Mehrez et al., *Ibid* **65**, 195419 (2002); Yong Chen et al., Appl. Phys. Lett., **82**, 1610 (2003)
 - [4] A. Nitzan and M. A. Ratner, Science, **300**, 1384 (2003)
 - [5] www.intel.com/research/silicon/mooreslaw.htm
 - [6] See, e.g., *Compound Semiconductor Surface Passivation and Novel Device Processing*, edited by H. Hasegawa et al., (MRS, Warrendale, Pennsylvania, 1999).
 - [7] M. A. Reed et al., Science **278**, 252 (1997).
 - [8] see R. F. Service, Science, **302**, 556 (2003)
 - [9] A. Turak et al., Appl. Phys. Lett. **81**, 766 (2002).
 - [10] M.C. Petty et al., Eds. *An Introduction to Molecular Electronics*, (Edward Arnold, London, 1995).
 - [11] D. Grozea et al., Appl. Phys. Lett. **81**, 3173 (2002).
 - [12] S. K. Kim et al., Mol. Cryst. Liq. Cryst. **377**, 133 (2002)
 - [13] M. G. Mason et al, J. App. phys. **89**, 2756 (2001) and references there in.
 - [14] W. J. H. van Gennip et al, J. Chem. Phys. **117**, 5031 (2002)
 - [15] N. D. Lang, Phys. Rev. B **34**, 5947 (1986)
 - [16] G. Kress, J. Furthmuller and J. Hafner, see <http://cms.mpi.univie.ac.at/vasp/>
 - [17] M. Kiguchi et al., Phys. Rev. Lett, **90**, 196803 (2003)
 - [18] For the acronyms, basis sets, etc., see: A.D. Becke, J.

- Chem. Phys., 98, 5648 (1993); C. Lee, W. Yang and R.G. Parr, Phys. Rev. B, 37,785 (1988).
- [19] *Gaussian 98*, Revision A.9, M. J. Frisch et al, Gaussian Inc., Pittsburgh, PA (1998).
- [20] M. W. C. Dharma-wardana and Marek Z. Zgierski, J. Opt. A: Pure Appl.Opt. 4, 278 (2002).